

**Long-lived coherent acoustic waves generated by femtosecond light pulses**I. Bozovic,<sup>1</sup> M. Schneider,<sup>2</sup> Y. Xu,<sup>3</sup> R. Sobolewski,<sup>3,4</sup> Y. H. Ren,<sup>5</sup> G. Lüpke,<sup>5</sup> J. Demsar,<sup>6</sup> A. J. Taylor,<sup>6</sup> and M. Onellion<sup>2</sup><sup>1</sup>Brookhaven National Laboratory, Upton, New York 11973-5000, USA<sup>2</sup>Department of Physics, University of Wisconsin, Madison, Wisconsin 53706, USA<sup>3</sup>Department of Electrical and Computer Engineering and Laboratory for Laser Energetics, University of Rochester, Rochester, New York, 14627-0231, USA<sup>4</sup>Institute of Physics, Polish Academy of Sciences, PL-02668 Warszawa, Poland<sup>5</sup>Department of Applied Science, College of William and Mary, Williamsburg, Virginia 23187, USA<sup>6</sup>Los Alamos National Laboratory, Los Alamos, New Mexico 87545, USA

(Received 16 October 2003; published 16 April 2004)

We report on photoexcitation of coherent longitudinal acoustic phonons in single-crystal cuprate thin films on epitaxially matched substrates. The photoinduced reflectance oscillations are unusually long lived; in some samples we could easily resolve them for hundreds of periods. We studied the effect of varying a number of parameters, including the film doping level, thickness, and temperature, as well as the pump and probe beam wavelength, power, polarization, and incidence angle. We account quantitatively for the oscillation period, dispersion, phase, and decay of amplitude with time.

DOI: 10.1103/PhysRevB.69.132503

PACS number(s): 78.47.+p, 43.35.+d, 63.20.Dj, 74.72.Dn

In transparent media, femtosecond light pulses generate coherent optical phonons via impulsive stimulated Raman scattering (ISRS).<sup>1</sup> In absorbing materials, the mechanism was initially ascribed to displacive excitation of coherent phonons (DECP)<sup>2</sup> and later to resonant ISRS.<sup>3</sup> Because of great interest in high-temperature superconductivity, cuprates have been studied extensively by ultrafast pump-probe techniques<sup>4-7</sup> and indeed photogeneration of coherent optical phonons has been reported.<sup>8</sup>

Coherent acoustic phonons have been photogenerated in nanoparticles and thin films as standing waves; the period of oscillations is proportional to the sample thickness.<sup>9,10</sup> Echoes of photo-generated acoustic pulses have been detected via intermittent changes in reflectance; this technique is renowned as picosecond ultrasonics or picosecond interferometry and has found a range of applications.<sup>11</sup> Thomsen *et al.*<sup>10</sup> also observed acoustic oscillations in a bulk sample of *a*-As<sub>2</sub>Se<sub>3</sub> and attributed this to oscillatory behavior of the sensitivity function, scanned by the traveling strain pulse.

Here, we report on the first observation of coherent longitudinal acoustic phonons in bilayer samples consisting of two complex oxides: a single-crystal cuprate thin film on epitaxially matched (titanate or aluminate) single-crystal substrate. The photoinduced reflectance oscillations are unusually long lived.

For the present study, we have synthesized a number of thin films of La<sub>2-x</sub>Sr<sub>x</sub>CuO<sub>4</sub> (LSCO) with *x* = 0, 0.15, and 0.30 and Bi<sub>2</sub>Sr<sub>2</sub>CuO<sub>6</sub> (Bi-2201) using atomic-layer molecular beam epitaxy (MBE). The films were atomically smooth and perfect, as deduced from the undamped oscillations of intensity of reflection high-energy electron diffraction (RHEED) during the growth as well as from subsequent film characterization by grazing-angle x-ray diffraction and atomic force microscopy.<sup>12</sup> This seems to play a role in the phenomena reported here; control experiments in less perfect films showed only strongly damped oscillations. The film thickness ranged from *d<sub>F</sub>* = 39 nm to *d<sub>F</sub>* = 78 nm. The femtosecond (~100 fs pulse width) pump/probe experiments

were performed and the results reproduced in three independent laboratories (W&M, UR, and LANL).

Figure 1 (main panel) illustrates the time-dependent change in reflectance ( $\Delta R/R$ ) from a metallic La<sub>2</sub>CuO<sub>4+ $\delta$</sub>  film, 52 nm thick, on SrTiO<sub>3</sub> (STO) substrate. These are the raw data as measured, except that 10 traces were averaged together. The pump pulse energy was 0.3  $\mu$ J, the repetition rate 250 KHz, the spot diameter 150  $\mu$ m, the fluence 1.6 mJ/cm<sup>2</sup>, and  $\lambda_{\text{pump}} = \lambda_{\text{probe}} = 800$  nm.

The initial part of the transient (not time resolved in Fig. 1) corresponds to the nonequilibrium dynamics of photoexcited carriers in the films; it has the shape and time duration

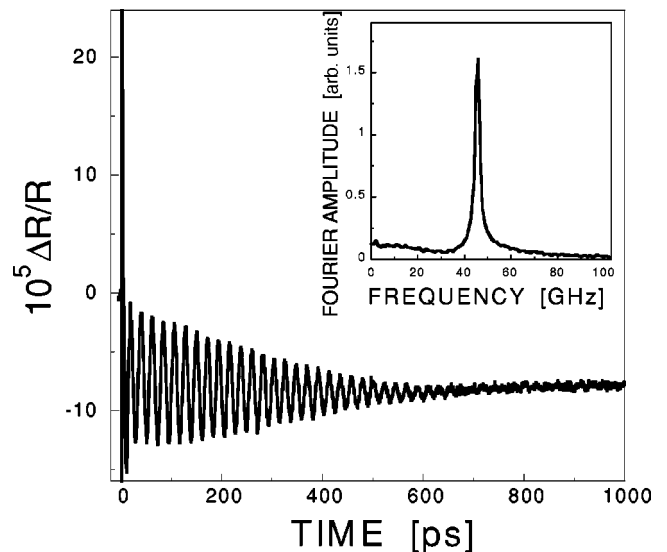


FIG. 1. Main panel: Oscillations in reflectance induced by a femtosecond light pulse in a metallic La<sub>2</sub>CuO<sub>4+ $\delta$</sub>  film on SrTiO<sub>3</sub> substrate. The pump fluence was 1.6 mJ/cm<sup>2</sup>, and  $\lambda_{\text{pump}} = \lambda_{\text{probe}} = 800$  nm. We have observed similar oscillations in other samples and with other pump/probe arrangements. Inset: The frequency spectrum obtained by applying FFT without any filtering or smoothing.

typical for the photoresponse of conducting oxides excited with femtosecond pulses,<sup>6</sup> and is not the subject of this work. Here we focus on the very regular oscillations that follow the initial transient and are superimposed on top of the thermal relaxation of acoustic phonons background. The period of these oscillations is two orders of magnitude longer than for optical phonons, indicating that these are acoustic vibrations. The Fourier transform (FFT) of the same data, plotted in Fig. 1 (inset), shows that the frequency is very sharply defined:  $\nu = 45.5 \pm 1$  GHz. Finally, the damping is remarkably weak; for some samples we could easily resolve hundreds of oscillations.

We studied the impact of a number of parameters, including the doping level (up to  $x = 0.30$ ) in  $\text{La}_{2-x}\text{Sr}_x\text{CuO}_4$  films, on both  $\text{SrTiO}_3$  and  $\text{LaSrAlO}_4$  substrates. For pumping, we also used  $\lambda_{\text{pump}} = 400$  nm, by frequency doubling. Using optical parametric amplifiers, we varied the probe beam wavelength from  $\lambda_{\text{probe}} = 400$  nm to  $\lambda_{\text{probe}} = 2110$  nm. The energy per pulse of the pump beam ranged from 0.02–50  $\mu\text{J}$  and the spot diameter from 100  $\mu\text{m}$  to 2 mm; this corresponds to a fluence of 0.02–20  $\text{mJ}/\text{cm}^2$ . The probe beam fluence was 10–100 times smaller. The incident angles  $\theta_{\text{pump}}$  and  $\theta_{\text{probe}}$  were varied between  $10^\circ$  and  $45^\circ$  with respect to the substrate normal. The findings were as follows.

Oscillations are (i) observed only in metallic films, (ii) pronounced only at relatively high pump fluence, and (iii) seen also in transmittance but much weaker, despite the much larger incoherent “background” signal. The period of oscillations  $\tau$  is not affected by changes in (iv) sample temperature  $T$  from 15 to 300 K, (v) the film thickness  $d_F$  by a factor of 2, (vi) the pump wavelength  $\lambda_{\text{pump}}$  by a factor of 2 (400 vs 800 nm), (vii) the pump or probe power density by a factor of 100, and (viii) the polarization of pump or probe light. However, (ix) the period scales with the probe wavelength, from  $\lambda_{\text{probe}} = 400$  nm to  $\lambda_{\text{probe}} = 2.1$   $\mu\text{m}$ . There is also (x) a weak dependence on the probe light incidence angle; for  $\theta_{\text{probe}} = 45^\circ$  the period is about 3% longer than for  $\theta_{\text{probe}} = 10^\circ$ . The amplitude of oscillations is not affected by changes in (xi) the pump wavelength  $\lambda_{\text{pump}}$  and (xii) the film thickness  $d_F$ . However, it (xiii) scales with the pump power  $P_{\text{pump}}$ , and (xiv) increases as  $\lambda_{\text{probe}}$  is decreased. (xv) The initial phase of oscillations  $\phi$  decreases as  $\lambda_{\text{probe}}$  is decreased, as shown in Fig. 2 (right scale). The damping of oscillations  $\Gamma$  is not affected by changes in (xvi) the doping level, (xvii) the film thickness  $d_F$  and (xviii) the sample temperature  $T$ , but (xviii) it increases as  $\lambda_{\text{probe}}$  is decreased.

In Fig. 2 (left scale), we plot the dependence of the oscillation frequency  $\nu$  on the probe beam wave vector  $k_{\text{probe}}$ ; here,  $\nu = 1/\tau$  and  $k_{\text{probe}} = 2\pi/\lambda_{\text{probe}}$ . The dispersion relation is nearly linear; together with the very low frequency (20–100 GHz), this indicates photogeneration of acoustic phonons. However, our finding (v) that  $\tau$  is independent of  $d_F$  excludes the standard explanation that assumes standing acoustic waves in the film, or a bouncing strain pulse.<sup>9,10</sup>

A simple physical model accounts quantitatively for these observations. In our experiments, the film absorbs  $10^{20}$ – $10^{22}$  photons/ $\text{cm}^3$  per pulse; this is comparable to the charge-carrier density ( $2$ – $4 \times 10^{21}$  holes/ $\text{cm}^3$ ) and causes significant electron heating. The photoexcited carriers ther-

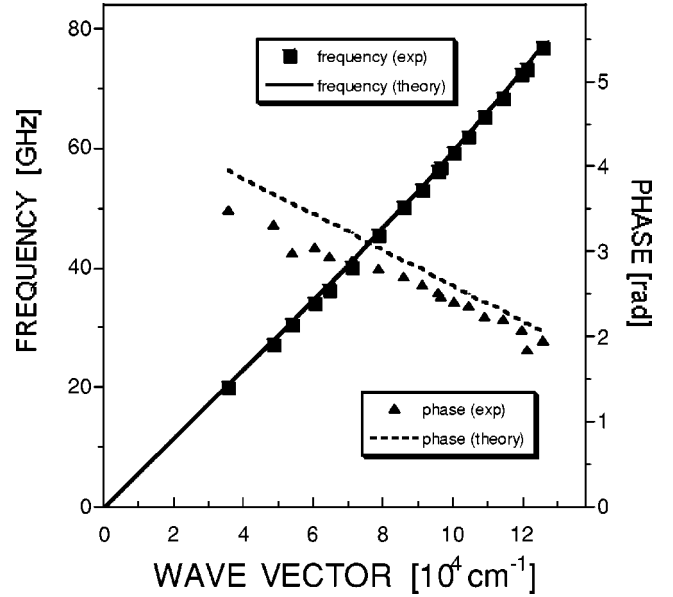


FIG. 2. Left scale: The frequency of oscillations as a function of the probe wave vector. Solid squares: the experimental data. Solid line: the predicted dependence  $\nu = (2n_s v_s \cos \theta / \pi) k_{\text{probe}}$ . There are no fitting parameters in this theory; we used the measured value for  $\theta$  and the tabulated values for  $n$  and  $v_s$ . Right scale: The phase of oscillations as a function of the probe wave vector, the experimental data (solid triangles), and the predicted dependence  $\phi = 3\pi/2 - (2nd_F)k_{\text{probe}}$  (dashed line).

malize within tens of femtoseconds and transfer the energy to the phonon system on a scale of hundred femtoseconds due to strong electron-optical phonon interaction.<sup>5</sup> The rapid rise in the phonon temperature  $T_{\text{ph}}$  leads to transient film expansion by 0.1–1%, mostly along the  $c$  axis since it is epitaxially constrained by the substrate. Thus, upon arrival of the pump pulse, the equilibrium ion positions are suddenly (on ps time scale) displaced by as much as 0.02  $\text{\AA}$ . The heat diffusion out of the film is limited by the acoustic phonon lifetime and the acoustic matching across the film-substrate interface and hence it is much slower—for cuprates typically on the order of ten nanoseconds.<sup>5</sup> The restitution force therefore changes abruptly at time  $t \approx 0$ . This is similar to DECP, except that the driving force is not a steplike change in the electron density but in the film temperature and therefore in the lattice density.

Clearly, this is not a special case of ISRS—the physics is qualitatively different here. ISRS is due to forward Raman scattering, for which  $q = n(k_i - k_f) = n\Omega/c$  is negligibly small. The phase velocity is equal to the speed of light inside the medium; the probe light sees all the atoms in the same phase, and the driving force is a  $\delta$  function in time and a step function in space.<sup>1</sup> In contrast, in our case the driving force is essentially completely localized in the film. Since  $d_F \ll \lambda_{\text{pump}}$ , we can approximate it as a step function in time and a  $\delta$  function in space, neglecting the film thickness. This perturbation generates coherent longitudinal acoustic phonons (CLAP’s) in the film, with the phase velocity equal to the speed of sound and with a finite  $q$ .

Our cuprate films are very thin and the CLAP momentum

bandwidth must be large. From  $\delta q \delta x > 1$  and  $\delta x \sim d_F \sim 50$  nm, we obtain  $\delta q > 2 \times 10^5$  cm<sup>-1</sup>, larger than the biggest  $k_{\text{probe}}$  we used. Hence, we expect to generate a broad band of CLAP's, comparable to the entire range of  $\lambda_{\text{probe}}$  accessible to us. The CLAP's are launched into the substrate as plane waves; they may be bunched together into a traveling strain pulse, as envisioned in the phenomenological theory of Thomsen *et al.*<sup>10</sup>

Turning now to the probe, the light pulse is very short and it takes a "snapshot" of the instantaneous phonon phase. The probe beam interacts with the material via several channels, including elastic scattering of photons on free electrons or phonons, phonon-assisted interband absorption, and backward Raman scattering. The last process is the weakest, but it is the one to provide a " $\lambda_{\text{probe}}$  filter:" the momentum selection rule is  $q = n(k_i + k_f) \approx 2nk_{\text{probe}}$ , and probe photons scatter exclusively on wavelength-matched CLAP's. The stimulated backward Raman scattering (SRS) is thus one candidate mechanism for the probe action. Another possibility, following Thomsen *et al.*,<sup>10</sup> is that the oscillations come from interference of the light beams reflected from the film, the substrate, and the strain pulse. Interestingly, both scenarios provide exactly the same formula for the dependence of  $\nu$  on  $k_{\text{probe}}$ , viz. the Eq. (1) below, and we cannot resolve this dichotomy experimentally at present. (One could differentiate between the two by spectroscopy in principle, but the Raman shift as small as what we have here, 1–3 cm<sup>-1</sup>, is extremely hard to resolve.)

In any case, within 5–10 ps the perturbation spreads into the substrate; hence, we expect  $2\pi/q = \lambda_{\text{probe}}/2n_s$ , where  $n_s$  is the index of refraction of the substrate. Taking into account the incident angle of probe beam  $\theta_{\text{probe}}$  we get  $q = 2n_s k_{\text{probe}} \cos \theta$  and hence

$$\nu = (n_s v_s \cos \theta / \pi) k_{\text{probe}}, \quad (1)$$

where  $\sin \theta = (1/n_s) \sin \theta_{\text{probe}}$  and  $v_s$  is the sound velocity in the substrate. This angular dependence is very weak; if  $\theta_{\text{probe}}$  is increased from 10° to 45°,  $\nu$  should decrease by about 4%—close to what we observed. Equation (1) dependence is plotted as the solid line in Fig. 2 (left scale). There are no fitting parameters in this theory—we used the measured value  $\theta_{\text{probe}} = 10^\circ$  (which corresponds to  $\theta = 4^\circ$ ) and the tabulated materials parameters: in SrTiO<sub>3</sub>,  $v_s = 7.8 \times 10^3$  m/s (Ref. 13) and  $n_s = [5.197 + 0.160k^2 / (39.5 - 0.0784k^2)]^{1/2}$  as determined from reflectance spectroscopy.<sup>14</sup> The weak dependence of  $n_s$  on  $k_{\text{probe}}$  causes a small departure from strict linearity in the dispersion relation. The agreement with our experimental data is outstanding, within 1–2%. The model also correctly explains observations (i)–(x), related to the occurrence of oscillations and their period.

As for the phase, let us for simplicity neglect the initial transient and consider interference of beams reflected from the three planes, representing the free film surface, the film/substrate interface, and the strain pulse that starts from the free surface, respectively. We infer that the oscillations should behave as  $\sin(\Theta t + \phi)$ , where

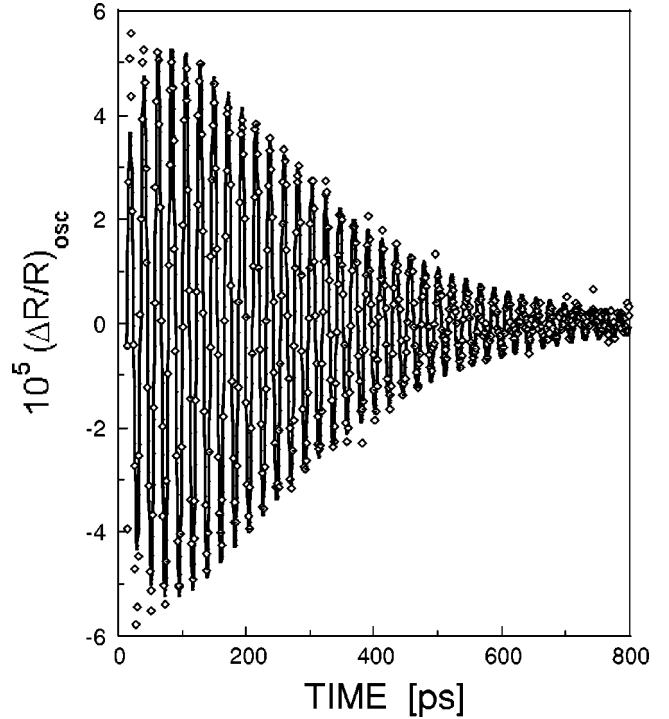


FIG. 3. Oscillations in reflectance, theory vs experiment. Open diamonds: the raw data as in Fig. 1, except that the initial transient and the background are subtracted and only every fourth data point is plotted. Thick solid line: the fit of the data to the function  $A(t) = A_0 \exp(-\Gamma t) \sin(\Omega t + \phi)$ . Note that  $\Omega$  and  $\phi$  are predicted from Eqs. (1) and (2), respectively; the only free parameters are  $A_0$  and  $\Gamma$ .

$$\phi = 3\pi/2 - (2n_s d_F) k_{\text{probe}}. \quad (2)$$

Inserting  $d_F = 52$  nm and using  $n_s \approx 2$  for LSCO, we get  $\phi = 4.7 - 0.21 k_{\text{probe}}$ , where  $k_{\text{probe}}$  is in  $(\mu\text{m})^{-1}$  and  $\phi$  is in radians. This function is plotted as a dashed line in Fig. 2 (right scale). Without any adjustable parameters, the agreement with the experimental data is within 10% or better for all wavelengths. It should be possible to improve this further by allowing for the spectral dependence of  $n_s$ , the actual shape of the acoustic wave, etc.

The amplitude of the oscillatory part of the reflectance  $A_0 = |\Delta R_0/R|_{\text{osc}}$ , scales as expected with the pump power, since  $\Delta R_0 \propto \delta n_f \propto \delta c_0 \propto \delta T_{\text{ph}} \propto P_{\text{pump}}$ ; here  $c_0$  is the lattice constant and  $n_f$  the index of refraction in the film. For a film very thin compared to the optical absorption depth  $d_F$  does not affect the local photon density and  $T_{\text{ph}}$ .

The damping we expect to be very weak, because the wave vectors of our CLAP's are very small, as is the phase space available to scattering on other phonons. A simple exponential damping of oscillations does not fit the data well; however, we get an excellent fit (see Fig. 3) using

$$A(t) = A_0 t^{1/2} \exp(-\Gamma t) \sin(\Omega t + \phi), \quad (3)$$

where  $A_0$  and  $\Gamma$  are the only free parameters while  $\Omega = 2\pi/\nu$  is given by Eq. (1) and  $\phi$  by Eq. (2). This dependence would be expected if CLAP's were probed via SRS. (The number of wavelengths grows as  $t$ , while the amplitude

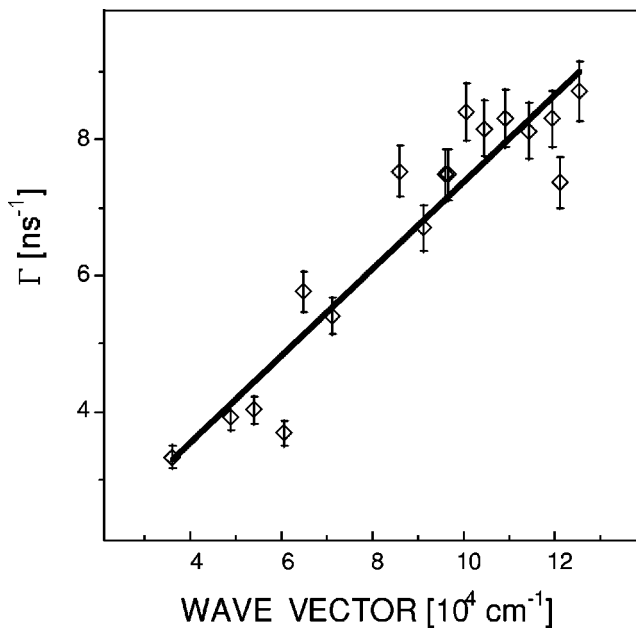


FIG. 4. The damping rate as a function of the wave vector of the probe beam.

falls off as  $1/\sqrt{t}$ . More experimental and theoretical studies are needed to clarify how significant is this finding. In Fig. 4 we show that the damping rate scales with the probe wave vector, as one would expect if say diffraction of CLAP's on nanometer-scale irregularities of the film/substrate interface played a major role.

We can suggest some possible applications. Manipulation of coherent phonons<sup>11</sup> could be extended to CLAP's in the

20–100 GHz range. Very long coherence time (up to several ns—hundreds of periods) that we have demonstrated could be of interest in all-optical computing. Ability to modulate in the GHz range the probe beam by fast pump pulses, in frames repeated, e.g., at 100 MHz, could be of interest for optical communications. Last but not least, one could build a source of monochromatic CLAP's. Let us consider, as an example, a trilayer structure consisting of a 50-nm-thick cuprate top layer, a 1.67- $\mu\text{m}$ -thick STO film, and a transparent oxide substrate lattice-matched but sonically mismatched to STO (e.g.,  $\text{CeO}_2$ ). This multilayer structure would create a sonic cavity, resonant for phonons with the wavelength  $\Lambda = \lambda_{\text{probe}}/2n = 167 \text{ nm}$  and the frequency  $\nu = 47 \text{ GHz}$ . Given the low damping, tens of passes should occur before attenuation. The cavity would support ten-wavelengths-long standing waves, and act as a coherent oscillator, with some CLAP's leaking out into the substrate. This device could operate as a source of monochromatic CLAP's, in the GHz range. One could even envision building a double (sonic and optical) cavity, capturing together both phonons and photons, and manipulating the photon-phonon interactions, such as was recently done in AlAs-AlGaAs superlattices (also grown by MBE).<sup>15</sup> Potential advantages of our scheme are in the magnitude of the effect, in perpendicular propagation (vertical devices), and in large lateral dimensions (mm or more).

We are grateful to H. Maris and K. A. Nelson for useful comments, and to the National Science Foundation, Air Force Office of Scientific Research and the U.S. Department of Energy (Contract No. DE-AC02-98CH10886) for support. Y.X. acknowledges Frank Horton Graduate Program in Laser Energetics.

<sup>1</sup>Y. X. Yan, E. B. Gamble, and K. A. Nelson, *J. Chem. Phys.* **83**, 5391 (1985); Y. X. Yan and K. A. Nelson, *ibid.* **87**, 6240 (1987); S. Ruhman, A. G. Joly, and K. A. Nelson, *IEEE J. Quantum Electron.* **24**, 460 (1988); W. A. Kutt, W. Albrecht, and H. Kurz, *ibid.* **28**, 2434 (1992).

<sup>2</sup>H. J. Zeiger *et al.*, *Phys. Rev. B* **45**, 768 (1992); A. V. Kuznetsov and C. J. Stanton, *Phys. Rev. Lett.* **73**, 3243 (1994).

<sup>3</sup>G. A. Garrett *et al.*, *Phys. Rev. Lett.* **77**, 3661 (1996); R. Merlin, *Solid State Commun.* **102**, 207 (1997); T. E. Stevens, J. Kuhl, and R. Merlin, *Phys. Rev. B* **65**, 144304 (2002).

<sup>4</sup>S. G. Han *et al.*, *Phys. Rev. Lett.* **65**, 2708 (1990).

<sup>5</sup>T. Gong *et al.*, *Phys. Rev. B* **47**, 14 495 (1993).

<sup>6</sup>L. Shi *et al.*, *Appl. Phys. Lett.* **64**, 1150 (1994).

<sup>7</sup>C. J. Stevens *et al.*, *Phys. Rev. Lett.* **78**, 2212 (1997); M. Lindgren *et al.*, *Appl. Phys. Lett.* **74**, 853 (1999); J. Demsar *et al.*, *Phys. Rev. Lett.* **82**, 4918 (1999); R. A. Kaindl *et al.*, *Science* **287**, 470 (2000); R. D. Averitt *et al.*, *Phys. Rev. B* **63**, 140502 (2001); M. L. Schneider *et al.*, *J. Europhys. Lett.* **60**, 460 (2002); G. P. Segre *et al.*, *Phys. Rev. Lett.* **88**, 137001 (2002); M. L. Schneider *et al.*, in *Superconducting and Related Oxides: Physics and Nanoengineering V*, edited by I. Bozovic and D. Pavuna (SPIE, Bellingham, 2002), pp. 174–181.

<sup>8</sup>J. M. Chwalek *et al.*, *Appl. Phys. Lett.* **57**, 1696 (1990); J. M.

Chwalek *et al.*, *ibid.* **58**, 980 (1991); W. Albrecht, Th. Kruse, and H. Kurz, *Phys. Rev. Lett.* **69**, 1451 (1992); O. V. Misochko, *Fiz. Tverd. Tela* **42**, 1169 (2000) [*Phys. Solid State* **42**, 1204 (2000)]; *Zh. Eksp. Theor. Phys.* **119**, 285 (2001) [*Phys. JETP* **92**, 246 (2001)]; A. I. Lobad and A. J. Taylor, *Phys. Rev. B* **64**, 180301 (2001).

<sup>9</sup>C. Thomsen *et al.*, *Phys. Rev. Lett.* **53**, 989 (1984).

<sup>10</sup>C. Thomsen *et al.*, *Phys. Rev. B* **34**, 4129 (1986).

<sup>11</sup>C. Thomsen *et al.*, *Opt. Commun.* **60**, 55 (1986); H. T. Grahn *et al.*, *Appl. Phys. Lett.* **53**, 2023 (1988); H. N. Lin *et al.*, *J. Appl. Phys.* **69**, 3816 (1991); L. Dhar *et al.*, *Chem. Rev. (Washington, D.C.)* **94**, 157 (1994); J. A. Rogers *et al.*, *Annu. Rev. Mater. Sci.* **30**, 117 (2000); H.-Y. Hao and H. J. Maris, *Phys. Rev. Lett.* **84**, 5556 (2000); *Phys. Rev. B* **63**, 224301 (2001).

<sup>12</sup>I. Bozovic *et al.*, *Phys. Rev. Lett.* **89**, 107001 (2002); I. Bozovic *et al.*, *Nature (London)* **422**, 873 (2003).

<sup>13</sup>*Landolt-Börnstein, Numerical Data and Functional Relations in Science and Technology, New Series III/28a* (Springer, Berlin, 1990), pp. 217 and 223.

<sup>14</sup>M. Cardona, *Phys. Rev.* **140**, A651 (1965).

<sup>15</sup>M. Trigo *et al.*, *Phys. Rev. Lett.* **89**, 227402 (2002); J. M. Warlock and M. L. Roukes, *Nature (London)* **421**, 803 (2003).